JOC Article

# Koopmans-Based Analysis of the Optical Spectra of *p*-Phenylene-Bridged Intervalence Radical Ions

Stephen F. Nelsen,*[,†] Michael N. Weaver,[†] João P. Telo,*[,‡] Brett L. Lucht,[§] and Stephen Barlow[⊥]

*Department of Chemistry, University of Wisconsin, 1101 University Avenue, Madison, Wisconsin 53706-1396, Instituto Superior Técnico, Química Orgânica, Av. Rovisco Pais, 1049-001 Lisboa, Portugal, Department of Chemistry, University of Rhode Island, Kingston, Rhode Island 02881, and School of Chemistry and Biochemistry, Georgia Institute of Technology, Atlanta, Georgia 30332-0400*

*nelsen@chem.wisc.edu; jptelo@ist.utl.pt*

*Received July 9, 2005*

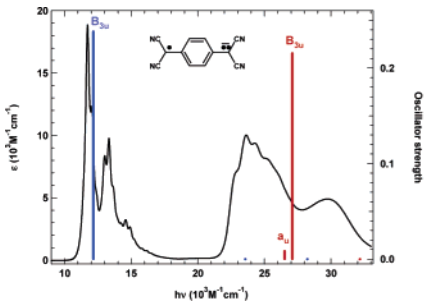



Simple interpretation of optical spectra of radical ions.

The optical spectra of 10 *p*-phenylene-bridged delocalized intervalence compounds $\mathbf{MC_6H_4M}^{\bullet-}$ or $^{\bullet+}$ are analyzed using the Koopmans-based method, which considers only transitions from filled orbitals to the singly occupied orbital (SOMO), called Hoijtink type A transitions, and from the SOMO to unoccupied orbitals, Hoijtink type B transitions, and ignores configuration interaction. The radical ions with quinonoid structures, those that form ring-**M** double bonds with **M** = $C(CN)_2$, $NMe_2$, 3-oxo-9-azabicyclo[3.3.1], $NPPh_3$, and O when the odd electron of the intervalence oxidation level is removed, are calculated to have the lowest-allowed type B transition lying mostly above the lowest-allowed A transition, with $B_i - A_j$ decreasing in the order shown from +14 370 to −1390 $cm^{-1}$, and the more intense second-lowest-allowed type B transition $B_i - A_j$ from +14 940 to +7070 $cm^{-1}$. The five radical anions with benzenoid structures, which form ring-**M** single bonds with **X** = CN, $CO_2Me$, CHO, $C_3HMeBF_2O_2$, and $NO_2$ when the odd electron of the intervalence oxidation level is removed, have a $B_i - A_j$ value of the opposite sign that increases in magnitude from −2880 to −17 050 $cm^{-1}$ in the order shown. Configuration interaction is of course present in the observed spectra, and the predictions ignoring it mostly overestimate transition energies by 1900−2600 $cm^{-1}$ for the quinonoid compounds (but by 450 $cm^{-1}$ for the M = $C(CN)_2$ radical anion), and by 1000−1400 $cm^{-1}$ for the benzenoid compounds (2500 $cm^{-1}$ for the M = CN radical anion). The very simple Koopmans-based model is useful for considering the optical spectra of these radical ions.

## Introduction

We consider here the optical spectra of radical ions **1**−**10** (see Scheme 1). All have a *p*-phenylene (1,4-benzenediyl) group bridging two "charge-bearing units", **M**. All are delocalized intervalence compounds (Robin-Day Class III);[1] that is, they have symmetrical charge distributions in their ground state (and therefore have charge on the bridge as well as at the **M** units), as demonstrated by the vibrational fine structure that is observed at least to some extent in the lowest-energy absorption band for each radical ion. Hush pointed out that when charge localization occurs in an intervalence radical ion, so that the **M** groups bear different charges, the lowest absorption band is a very broad, nearly

[†] University of Wisconsin.
[‡] Instituto Superior Técnico.
[§] University of Rhode Island.
[⊥] Georgia Institute of Technology.

(1) Robin, M. B.; Day, P. *Adv. Inorg. Chem.* **1967**, *10*, 247−422.



10.1021/jo0514218 CCC: $30.25 
Published on Web 10/13/2005

**SCHEME 1. Structures of the Radical Ions Studied**

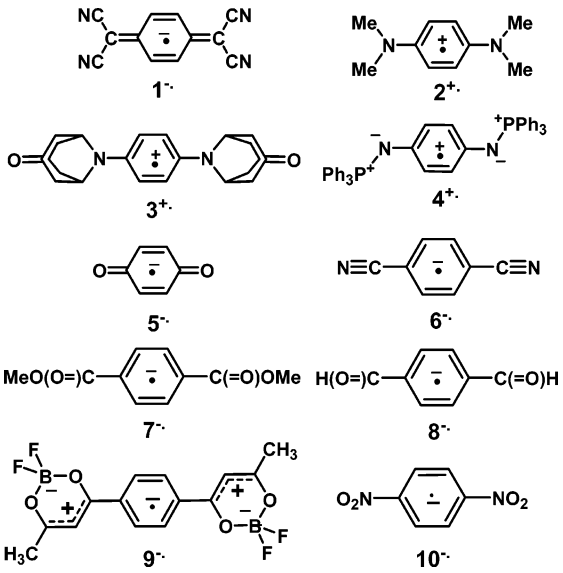


Gaussian-shaped peak that corresponds to charge transfer between the **M** groups, such as $\mathbf{M}^{+}-\mathbf{B}-\mathbf{M} \rightarrow \mathbf{M}-\mathbf{B}-\mathbf{M}^{+}$, and that the two-state model is useful: charge localization occurs when the Marcus vertical reorganization energy ($\lambda$) is greater than twice the electronic coupling between the **M** groups ($V_{ab}$).[2] The *p*-phenylene group is one of the better coupling units; that is, it causes large $V_{ab}$ values, and the only organic charge-bearing unit for which charge localization has been demonstrated to occur with the *p*-phenylene linker is bis(hydrazine) radical cation $\mathbf{A}^{+}$.[3]

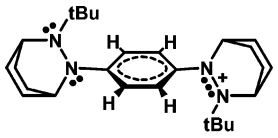


$\mathbf{A}^{\bullet+}$

It has been known for 20 years that single-point calculations with a neutral charge performed at radical cation geometries (neutral in cation geometry, or NCG) can be utilized to estimate the lowest transition energy in the optical spectra of the radical cations,[4] and are often very successful even when there is a very large geometry change between the neutral compound and the radical cation, as occurs for hydrazines.[5] Filling the singly occupied molecular orbital (SOMO) by adding one electron allows for the application of Koopmans' theorem, which states that orbital energies are the negative of ionization potentials.[6] The energy gap between the NCG SOMO and the lower-energy filled orbitals proves to be close to the transition energies for the filled orbital to

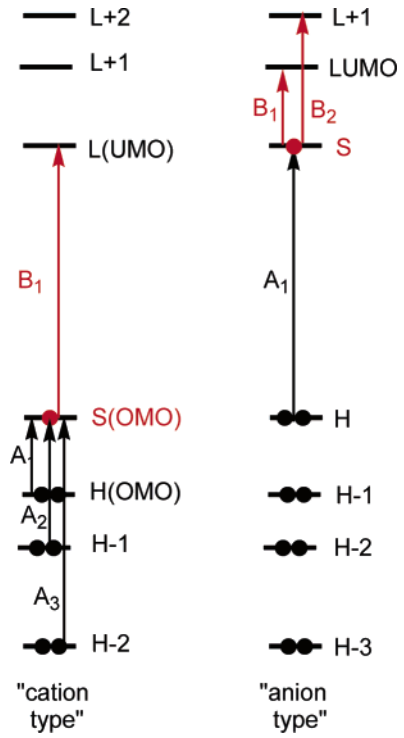


**FIGURE 1.** Cartoon representation of Hoijtink type A and B transitions for radical cation and radical anion alternate hydrocarbons.

SOMO transitions of the radical cation, which we will follow Bally[7] in calling Hoijtink[8] type A transitions.[9] More properly, type A transitions involve the promotion of an electron from the filled $\beta$ orbitals to the lowest unoccupied $\beta$ orbital. Other important transitions in radical ions are from the SOMO to virtual (unoccupied) orbitals, the Hoijtink type B transitions, which are also called non-Koopmans transitions by Bally. A more proper description of type B transitions is that they involve promotion of the α highest occupied molecular orbital to virtual α orbitals. The origins of these type A and B transitions are depicted in cartoon form in Figure 1. If the principal thing that makes NCG calculations give orbital energy gaps that are close to transition energies for type A transitions of radical cations is that the orbital occupancy is the same for the origin and destination orbitals, the corresponding calculation for type B transitions would involve a calculation at the radical ion geometry with an empty SOMO (dication in cation geometry, or DCG, for radical cations, neutral in anion geometry, or NAG, for radical anions). We recently pointed out that NAG calculations are successful for predicting the $B_1$ band energies for some delocalized dinitroaromatic radical anions.[10] Because most radical ions have both type A and

(2) Hush, N. S. *Prog. Inorg. Chem.* **1967**, *8*, 391−444.
(3) (a) Nelsen, S. F.; Ismagilov, R. F.; Powell, D. R. *J. Am. Chem. Soc.* **1996**, *118*, 6313−6314. (b) Nelsen, S. F.; Ismagilov, R. F.; Powell, D. R. *J. Am. Chem. Soc.* **1997**, *119*, 10213−10222.
(4) Nelsen, S. F.; Blackstock, S. C.; Yumibe, N. P.; Frigo, T. B.; Carpenter, J. E.; Weinhold, F. *J. Am. Chem. Soc.* **1985**, *107*, 143−149.
(5) Nelsen, S. F.; Tran, H. Q.; Ismagilov, R. F.; Chen, L.-J.; Powell, D. R. *J. Org. Chem.* **1998**, *63*, 2536−2543.
(6) Koopmans, T. *Physica* **1934**, *1*, 104−113.
(7) Bally, T. In *Radical Ionic Systems*; Lund, A., Shiotani, M., Eds.; Kluwer: Dortrecht, The Netherlands, 1991; pp 3−54.
(8) (a) Hoijtink, G. J.; Weijland, W. P. *Recl. Trav. Chim. Pays-Bas* **1957**, *76*, 836−838. (b) Buschow, K. J. J.; Dieleman, J.; Hoijtink, G. J. *Mol. Phys.* **1963**−**1964**, *7*, 1−9.
(9) The transition energies thus calculated include forbidden transitions that cannot be observed, so a way of estimating the oscillator strengths is needed, and was supplied by Clark for semiempirical calculations. See: Clark, T.; Teasley, M. F.; Nelsen, S. F.; Wynberg, H. *J. Am. Chem. Soc.* **1987**, *109*, 5719−5724.
(10) Nelsen, S. F.; Konradsson, A. E.; Telo. J. P. *J. Am. Chem. Soc.* **2005**, *127*, 920−925.

type B transitions as strong bands, it is necessary to calculate both to understand the optical spectra of radical ions. These Koopmans-based calculations involve the simplest model for consideration of optical absorption spectra; they include no configuration interaction (CI). One reason it took so long to discover the Koopmans-based method for type B transitions is that errors are quite large with semiempirical calculations. We show in this work that Koopmans-based estimations are more successful with B3LYP hybrid Hartree−Fock density functional theory calculations (and note here that they are not useful with Hartree−Fock calculations that include no electron correlation).

## Computational Methodology

All radical ion geometries were optimized using standard gradient methods in Spartan'02.[11] The band intensities in this model are available from the dipole matrix, which may be printed using keyword DIMO in Weinhold's NBO program.[12] The Gaussian 98 program suite[13] was used for all single-point calculations requiring the use of NBO 5.0. All calculations employed the standard Pople style 6-31G* or 6-31+G* basis sets as implemented in Spartan and Gaussian, and the B3LYP[14] density functional was applied in each case.

## Results

Optical spectra have been determined in dimethylformamide (for **1**$^{\bullet-}$, **5**$^{\bullet-}$ −**8**$^{\bullet-}$, and **10**$^{\bullet-}$), tetrahydrofuran (for **9**$^{\bullet-}$), acetonitrile (for **2**$^{\bullet+}$ and **3**$^{\bullet+}$), or methylene chloride (for **4**$^{\bullet+}$), and are compared with Koopmans-based calculations in Figures 2−11. The optical spectra of **1**$^{\bullet-}$ and **5**$^{\bullet-}$−**8**$^{\bullet-}$ were determined in this work. We previously discussed the spectra of **2**$^{\bullet+}$ and **3**$^{\bullet+}$ in terms of the two-state model (now shown to be inappropriate for delocalized intervalence compounds),[15] and have discussed the resonance Raman spectrum of **3**$^{\bullet+}$.[16] Lucht and co-workers studied the properties and optical spectrum of

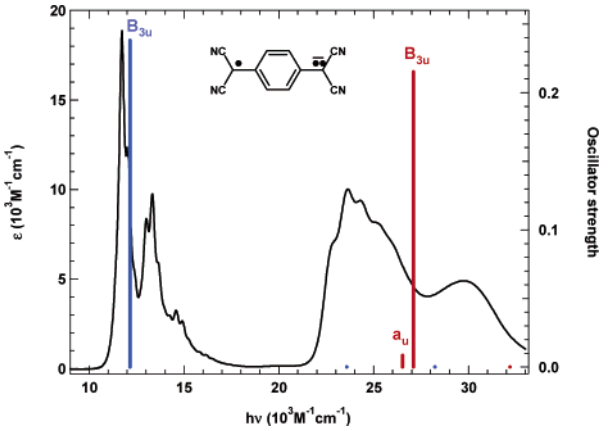


**FIGURE 2.** Optical absorption spectrum of **1**$^{\bullet-}$ with calculated type A (blue sticks) and type B (red sticks) transition energies and oscillator strengths superimposed.

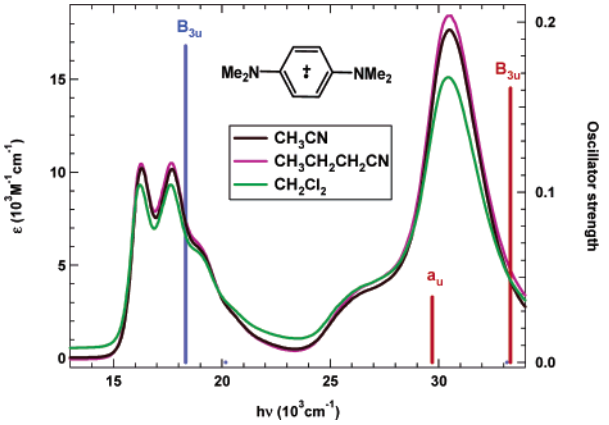


**FIGURE 3.** Same as Figure 2 for **2**$^{\bullet+}$ in three solvents.

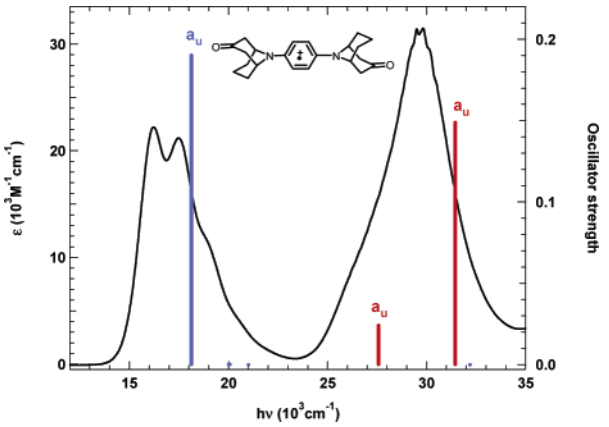


**FIGURE 4.** Same as Figure 2 for **3**$^{\bullet+}$.

**4**$^{\bullet+}$, and showed that it is oxidized at approximately the same potential as a *p*-phenylene diamine derivative,[17] and Barlow and co-workers studied the *p*-phenylene-bis(dioxaborine) radical anion **9**$^{\bullet-}$.[18] We recently discussed in detail the spectra of dinitroaromatic radical anions, including **10**$^{\bullet-}$.[19] Figures 2−11 show the optical spectra for these compounds, with stick spectra showing the

(11) *Spartan'02*, Wavefunction, Inc.: Irvine, CA, 2002.
(12) (a) Glendening, E. D.; Badenhoop, J. K.; Reed, A. E.; Carpenter, J. E.; Bohmann, J. A.; Morales, C. M.; Weinhold, F. *NBO,* version 5.0; Theoretical Chemistry Institute, University of Wisconsin: Madison, WI, 2001. (b) We used the implementation in Gaussian, which is available at Wisconsin; the NBO provided with Gaussian is an older version that does not include the DIMO keyword.
(13) Frisch, M. J.; Trucks, G. W.; Schlegel, H. B.; Scuseria, G. E.; Robb, M. A.; Cheeseman, J. R.; Zakrzewski, V. G.; Montgomery, J. A., Jr.; Stratmann, R. E.; Burant, J. C.; Dapprich, S.; Millam, J. M.; Daniels, A. D.; Kudin, K. N.; Strain, M. C.; Farkas, O.; Tomasi, J.; Barone, V.; Cossi, M.; Cammi, R.; Mennucci, B.; Pomelli, C.; Adamo, C.; Clifford, S.; Ochterski, J.; Petersson, G. A.; Ayala, P. Y.; Cui, Q.; Morokuma, K.; Malick, D. K.; Rabuck, A. D.; Raghavachari, K.; Foresman, J. B.; Cioslowski, J.; Ortiz, J. V.; Baboul, A. G.; Stefanov, B. B.; Liu, G.; Liashenko, A.; Piskorz, P.; Komaromi, I.; Gomperts, R.; Martin, R. L.; Fox, D. J.; Keith, T.; Al-Laham, M. A.; Peng, C. Y.; Nanayakkara, A.; Gonzalez, C.; Challacombe, M.; Gill, P. M. W.; Johnson, B.; Chen, W.; Wong, M. W.; Andres, J. L.; Gonzalez, C.; Head-Gordon, M.; Replogle, E. S.; Pople, J. A. *Gaussian 98 A.9*; Gaussian, Inc.: Pittsburgh, PA, 1998.
(14) (a) Becke, A. D. *J. Chem. Phys.* **1993**, *98*, 5648. (b) Becke, A. D. *Phys. Rev. A* **1988**, *38*, 3098. (c) Lee, C.; Yang, W.; Parr, R. G. *Phys. Rev. B* **1988**, *37*, 785. (d) Vosko, S. H.; Wilk, S. H.; Nusair, M. *Can. J. Phys.* **1980**, *58*, 1200.
(15) Nelsen, S. F.; Tran, H. Q. *J. Phys. Chem. A* **1999**, *103*, 8139−8144.
(16) Bailey, S. E.; Zink, J. I.; Nelsen, S. F. *J. Am. Chem. Soc.* **2003**, *125*, 5939−5947.
(17) Escobar, M.; Jin, Z.; Lucht, B. L. *Org. Lett.* **2002**, *4*, 2213−2216.
(18) Risko, C.; Barlow, S.; Coropceanu, V.; Halik, M.; Brédas, J.-L.; Marder, S. R. *Chem. Commun.* **2003**, 194−195.

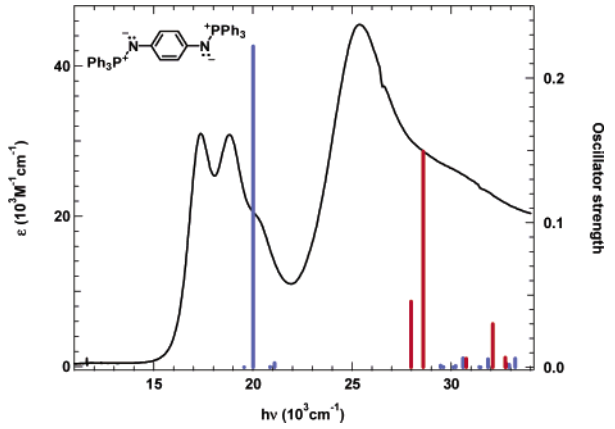


**FIGURE 5.** Same as Figure 2 for $\mathbf{4}^{\bullet+}$.

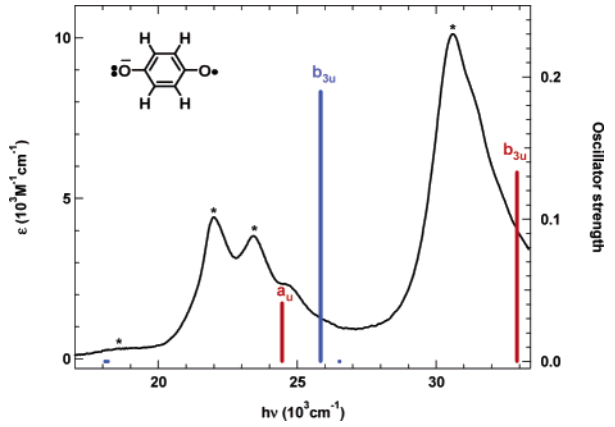


**FIGURE 6.** Same as Figure 2 for $\mathbf{5}^{\bullet-}$. The asterisks mark the energies reported in the Supporting Information, S6.

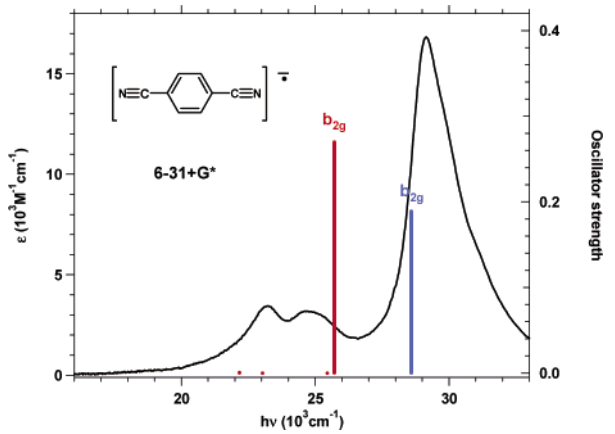


**FIGURE 7.** Same as Figure 2 for $\mathbf{6}^{\bullet-}$.

Koopmans-based transition energies (blue for type A bands, red for type B) and the heights of the sticks representing the calculated oscillator strengths (values shown on the right-hand axis). Solvent changes cause only small differences in optical spectra for delocalized intervalence compounds, although this is shown here only for $\mathbf{2}^{\bullet+}$, for which spectra in methylene chloride, butyronitrile, and acetonitrile are plotted.[15] The band shapes

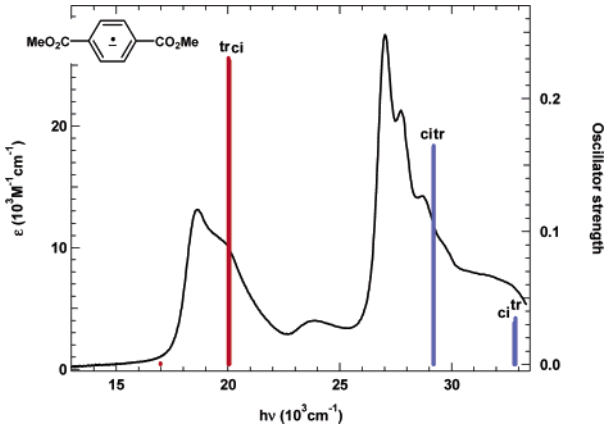


**FIGURE 8.** Same as Figure 2 for $\mathbf{7}^{\bullet-}$.

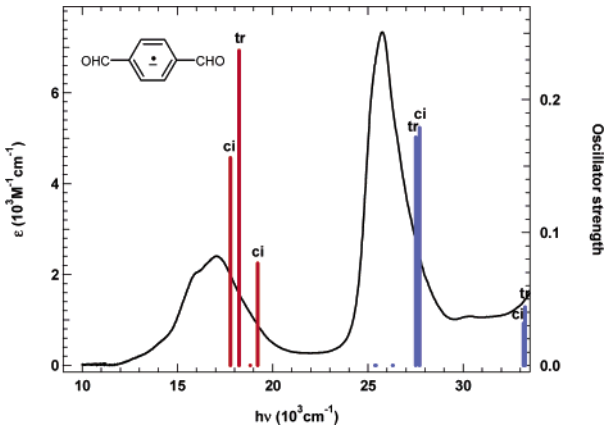


**FIGURE 9.** Same as Figure 2 for $\mathbf{8}^{\bullet-}$.

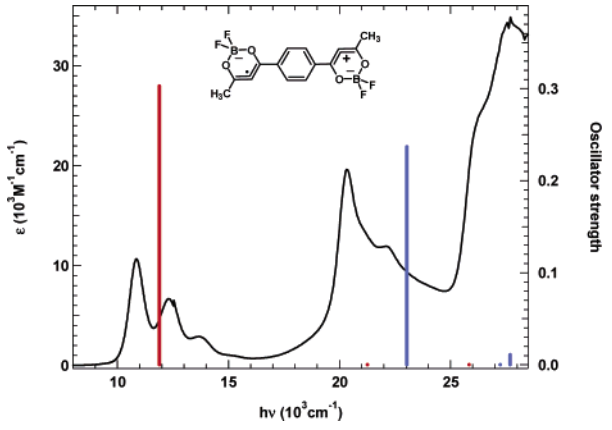


**FIGURE 10.** Same as Figure 2 for $\mathbf{9}^{\bullet-}$.

and positions in these solvents are nearly indistinguishable. The differences in $\epsilon$ are not reliable because of the small amounts weighed out in making up the solutions.

Table 1 summarizes some properties of these radical ions. The systems studied have 1−35 atom charge-bearing units, some of which contain extended $\pi$ orbitals and some of which do not, so the **M** units cover a broad range of structures. The compounds were numbered in a way that corresponds to the decreasing differences in energy between the allowed type B and type A orbitals, which covers a span of 32 000 $cm^{-1}$ (3.97 eV).

(19) Nelsen, S. F.; Weaver, M. N.; Telo, J. P.; Zink, J. I. *J. Am. Chem. Soc.* **2005**, *127*, 10611−10622.

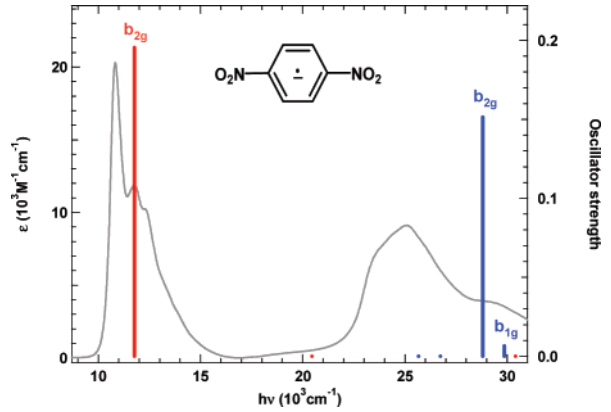


**FIGURE 11.** Same as Figure 2 for **10**•−.

**TABLE 1. Some Properties of Delocalized Intervalence Radical Ions 1−10**

| compd. | M | M atoms | allowed $B_i - A_i$ | molec. symmetry | SOMO symmetry |
|---|---|---|---|---|---|
| | | Quinoid Compounds[a] | | | |
| **1**•− | $(CN)_2C$ | 5 | +14370, +14940 | $D_{2h}$ | $b_{2g}$ |
| **2**•+ | $NMe_2N$ | 9 | +11380, +14980 | $D_{2h}$ | $b_{2g}$ |
| **3**•+ | k33N[b] | 22 | +9450, +13320 | $C_i$ | $a_g$ |
| **4**•+ | $Ph_3PN$ | 35 | +7960, +8580 | $C_2$ | b |
| **5**•− | O | 1 | −1390, +7070 | $D_{2h}$ | $b_{2g}$ |
| | | Benzenoid Compounds[a] | | | |
| **6**•− | CN | 2 | −2880 | $D_{2h}$ | $b_{3u}$ |
| **7**•− | $CO_2Me$ | 7 | −9150, −9150 | $C_{2h}$,$C_{2v}$ | $a_u$, $b_1$ |
| **8**•− | CHO | 3 | −9260, −9930 | $C_{2h}$,$C_{2v}$ | $a_u$, $b_1$ |
| **9**•− | $C_3HMeBF_2O_2$ | 12 | −11150 | $C_1$ | |
| **10**•− | $NO_2$ | 3 | −17050 | $D_{2h}$ | $b_{3u}$ |

[a] At the oxidation level with the odd electron removed. [b]k33N is an abbreviation for the 9-azabicyclo[3.3.1]nonan-3-one-9-yl group.

## Discussion

The comparisons in this paper were principally carried out to establish whether Koopmans-based calculations are generally useful for analysis of the optical spectra of radical ions. The low-energy regions of these spectra appear to be qualitatively rather well-described by these simple calculations. Virtually all of the calculated transition energies are too large, partly because the calculations are for the gas phase and solvation lowers the transition energies for the lower bands, but also because configuration interaction is ignored. Of course, CI will occur between transitions of the same symmetry, and Hoijtink type C bands (transitions from filled orbitals to virtual orbitals) will also contribute to these spectra, as may be calculated using the currently popular time-dependent density functional theory method, TD-DFT, which takes (for the first five transitions) more than an order of magnitude longer to carry out than Koopmans-based single-point calculations for most of the compounds studied. However, as is documented in the Supporting Information, the band positions are predicted to be closer to the experimental values using Koopmans-based calculations that ignore configuration interaction than they are by using TD-DFT. This was also pointed out in our paper on dinitroaromatic radical anions.[19]

The compounds studied clearly fall into two classes. **1**−**5** are structurally related to *p*-benzoquinone, **5**, with two C=C, C=N, or C=O double bonds when an electron is removed from the radical ion oxidation level, producing neutral compounds for **1** and **5**, and dications for **2**−**4**. We will refer to these radical ions as quinonoid. The remaining compounds, those from **6**−**10**, are benzenoid, that is, they are p-disubstituted benzene derivatives in their neutral oxidation level, with single bonds between the 1,4-carbons and their substituents. Qualitatively, by assigning six $\pi$ electrons to the benzene ring in each case, we will determine the quinonoid intervalence compounds **1**•−, **2**•+−**4**•+, and **5**•− to have three electrons in the p-rich orbitals at the atoms attached to the benzene ring (or delocalized onto groups attached to it), whereas the benzenoid intervalence compounds **6**•−−**10**•− have a single antibonding electron in the pair of **M** groups. This leads to the expectation that the lowest-energy transition for the quinonoid compounds ought to be the filled orbital to SOMO, i.e., Hoijtink type A, and that for the benzenoid compounds should be SOMO to unfilled, or Hoijtink type B. This is almost what is calculated, but as shown in Figure 6, a type B transition is calculated at lower energy than the type A for **5**•−, and the energy gap between type A and B transitions is unusually small for **6**•−, although a similar inversion is not calculated to occur in this case. A more-quantitative analysis is needed to understand these optical spectra better. Nelsen and Zink have developed the neighboring orbital analysis for the purpose of extracting electronic couplings from the optical spectra of delocalized intervalence compounds, and have applied it quantitatively thus far to dinitroaromatic radical anions (including **10**•−),[19] and to radical cations related to tetraalkylbenzidines.[20] In this work we will consider only its qualitative aspects, that the **M** group orbitals mix most strongly with the bridge orbitals of proper symmetry that are closest in energy, so the symmetric and antisymmetric **M** and bridge diabatic orbitals form a set of four neighboring orbitals that can have one to seven electrons for the delocalized intervalence compounds under discussion.

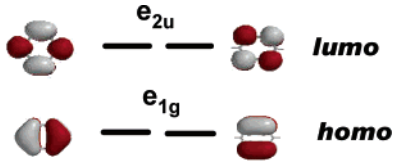


**FIGURE 12.** Neighboring $\pi$ orbitals of benzene for interaction with the **M** orbitals of *p*-phenylene intervalence compounds.

The **M** p-rich atomic orbitals at the atoms connected to $C_1$ and $C_4$ of the benzene ring have a vanishingly small direct overlap, so in the diabatic basis they appear as an equal energy pair of orbitals that are related by being either symmetric or antisymmetric with respect to a plane bisecting the molecules. The pair of **M** p-rich orbitals interact significantly only with benzene $\pi$ orbitals (shown in Figure 12) that have density at $C_1$ and $C_4$, so they do not interact with those shown at the right of Figure 12. The antisymmetric **M** pair interacts with the $e_{1g}$ HOMO and the symmetric pair with the $e_{2u}$ LUMO shown at the left side of Figure 12. Of course, the

(20) Nelsen, S. F.; Luo, Y.; Weaver, M. N.; Lockard, J. V.; Zink, J. I. Beyond the Two-State model: Optical Spectra of Protected Diamine Intervalence Radical Cations Related to N,N,N′,N′-Tetraalkylbenzidine; under review.

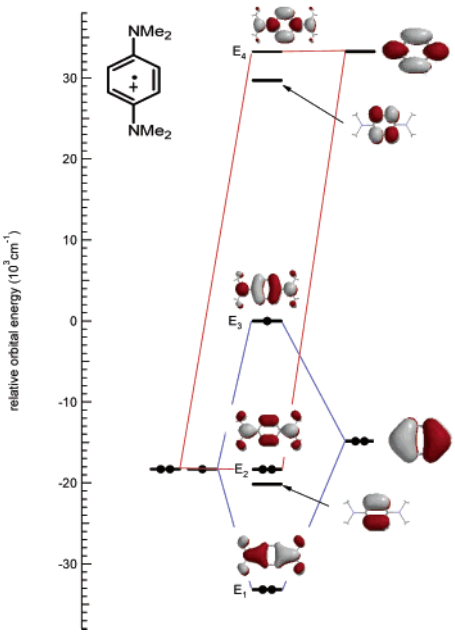


**FIGURE 13.** Diabatic and adiabatic neighboring orbitals for **2**$^{\bullet+}$. The ring-centered adiabatic orbitals that have a node through the 1,4-bonds and hence do not interact significantly are also shown, but the electrons in the occupied orbital are not.

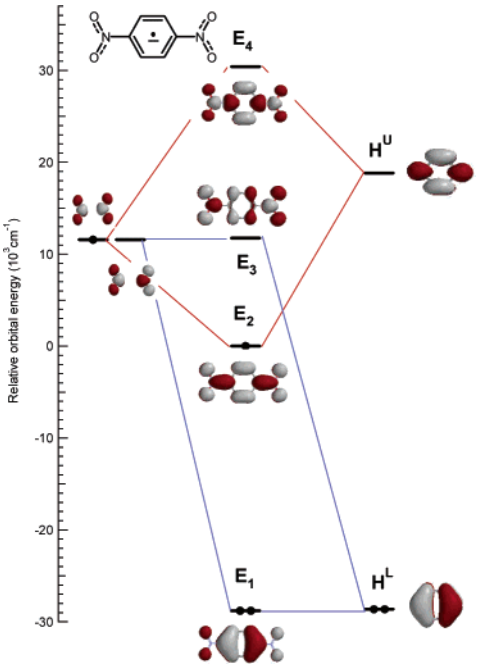


**FIGURE 14.** Diabatic and adiabatic neighboring orbitals for **10**$^{\bullet-}$.

symmetric **M** p-rich orbital pair actually interacts with all symmetric benzene orbitals that have significant overlap, but the interaction is greatest with the orbitals that are closest in energy. The zero node $a_{2u}$ benzene $\pi$ orbital is closer in energy to the $e_{1g}$ HOMO than to the $e_{2u}$ LUMO of benzene, but the heteroatom substitution in these compounds moves this orbital away, so that the *p*-phenylene orbitals resembling benzene HOMO and LUMO shown are the neighboring orbitals in all cases considered here. Benzoquinone radical anion (**5**$^{\bullet-}$) is calculated to have the lowest-energy diabatic **M** orbitals of the compounds discussed here, so it might be expected to have the most important mixing with the nodeless $e_{2u}$ benzene $\pi$ orbital. For **5**$^{\bullet-}$, Koopmans-based calculations get the energy of the $B_3$ adiabatic orbital (that mixed with the $e_{2u}$ orbital shown in Figure 12) at +4.22 eV and the $A_9$ adiabatic orbital (that mixed with the $a_{2u}$ benzene $\pi$ orbital) at −6.86 eV relative to the SOMO.

Because the **M** orbitals are 3/4 filled for the quinonoid compounds, and are heteroatom centered, their diabatic combination orbital energies lie much closer to the antisymmetric *p*-phenylene HOMO than to the symmetric LUMO of Figure 12. This makes the electronic interaction of the antisymmetric **M** combination orbital much greater than that of the symmetric one, leading to the pattern of adiabatic orbitals shown in Figure 13, a five-electron neighboring orbital system with an antisymmetric SOMO. Conversely, because there is only one electron in the two **M** orbitals for the benzenoid compounds, their energy is closer to that of the benzene LUMO than to that of the HOMO of Figure 12, causing significantly greater mixing with the LUMO. This makes the symmetric ring-**M** bonding adiabatic combination orbital lie significantly lower than the nearly unmixed ring-**M** antibonding antisymmetric adiabatic orbital, producing a three-electron neighboring orbital system with a symmetric SOMO (see Figure 14, where the orbitals for **10**$^{\bullet-}$ are illustrated).

The considerations discussed above are quite general, because all of the quinonoid intervalence compounds have five-electron neighboring orbital systems, with closely related SOMO orbitals that are $b_{2g}$ in $D_{2h}$ symmetry, and all of the benzenoid ones have three-electron ones and SOMO orbitals that are $b_{3u}$ symmetry in $D_{2h}$ symmetry), as shown by the SOMO electron density orbital diagrams in Figure 15.

One type A and two type B bands are predicted in the low-energy spectral region considered for the quinonoid compounds **1**$^{\bullet-}$ to **5**$^{\bullet}$, although the lower-energy type B transition (the $a_u$ band for the $D_{2h}$ examples) is calculated to be rather weak. In contrast, there are only two allowed transitions predicted for the benzenoid systems **6**$^{\bullet-}$ −**10**$^{\bullet-}$. The Koopmans-based band positions, intensities, and deviations from experimental values are shown in Table 2. Orbital symmetries for the transition origin (for type A) or terminus (for type B) for the $D_{2h}$ systems reveal the most because they allow us to see which transitions must mix because they have the same symmetry.

The quinonoid intervalence compounds are mostly characterized by type A lowest-energy bands, but for the benzoquinone radical anion, the type A band lies between the two allowed type B bands. The first band must therefore consist of two transitions, although vibrational fine structure is seen, suggesting that despite configuration interaction that shifts the bands substantially (the deviations for the lowest-energy bands of **4**$^{\bullet-}$−**6**$^{\bullet-}$ are the largest, at about 2500 cm$^{-1}$, suggesting that configuration interaction effects are largest for these compounds), the calculated transition-energy difference of 1390 cm$^{-1}$ is close to the actual separation of the bands, so that their fine structure overlaps and the first band has both type

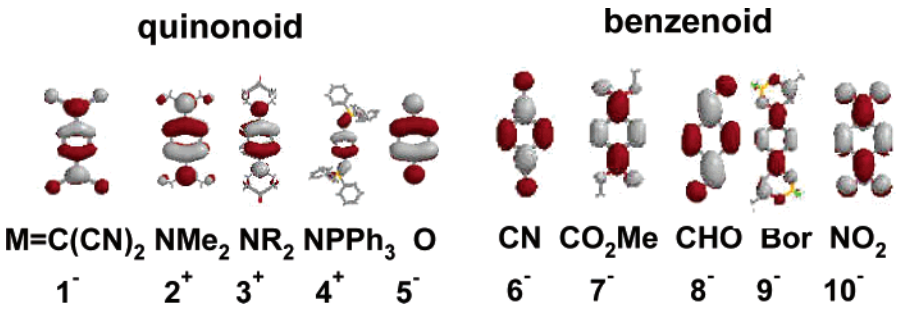


**FIGURE 15.** Electron density diagrams of the SOMO for **1**•− −**10**•−.

**TABLE 2. Koopmans-based Transition Energy Predictions and Shifts from Experimental Values**

| compd. | M | SOMO system | band 1[a] | $\Delta E$[b] | band 2[a] | $\Delta E$[b] | band 3[a] | $\Delta E$[b] |
|---|---|---|---|---|---|---|---|---|
| **1**•− | $(CN)_2C$ | $b_{2g}$ | 12 150 (0.24) [$A_1$ ($b_{3u}$)] | +450[c] | 26 520 (0.01) [$B_1$ ($a_u$)] | +2900 (−3200) | 27 090 (0.22) [$B_2$ ($b_{3u}$)] | +4200 (−2600) |
| **2**•+ | $Me_2N$ | $b_{2g}$ | 18 330 (0.19) [$A_1$ ($b_{1u}$)] | +2030[d] | 29 710 (0.04) [$B_1$ ($a_u$)] | +∼2900 | 33 310 (0.16) [$B_2$ ($b_{1u}$)] | +2800 |
| **3**•+ | k33N | $a_g$ | 18 190 (0.19) | +1930[e] | 27 580 (0.02) | no max. | 31 450 (0.15) | +1850 |
| **4**•+ | $PPh_3N$ | | 20 010 (0.22) | +2610[f] | 27 970 (0.05) | no max. | 28 590 (0.15) | +3190 |
| **5**•− | O | $b_{2g}$ | 24 450 (0.04) [$B_1$ ($a_u$)] | +2450[c] | 25 840 (0.19) [$A_3$ ($b_{3u}$)] | +2400 | 32 910 (0.13) [$B_2$ ($b_{3u}$)] | +2300 |
| **6**•− | CN | $b_{3u}$ | 25 710 (0.27) [$B_5$ ($b_{2g}$)] | +2500[c] | 28 590 (0.19) [$A_1$ ($b_{2g}$)] | −600 | | |
| **7**•− | $CO_2Me$ | $a_u$ | 20 030 (0.23) [$B_2$] | +1430[c] | 29 180 (0.16) [$A_2$] | +2180 | | |
| **8**•− | C(=O)H | $a_u$ | 18 240 (0.24) [$B_{1,2}$(ci),$B_2$(tr)] | +1240[c] | 27 500 (0.17) [$A_3$ (both)] | +1700 | | |
| **9**•− | $C_3HMeBF_2O_2$ | − | 11 890 (0.30) [$B_1$] | +990[g] | 23 040 (0.24) [$A_1$] | +2740 | | |
| **10**•− | $NO_2$ | $b_{3u}$ | 11 770 (0.20) [$B_1$ ($b_{2g}$)] | +970[h] | 28 820 (0.15) [$A_3$ ($b_{2g}$)] | +3720 | | |

[a] The numbers given are $h\nu$ ($cm^{-1}$), with frequency $f$ in parentheses, Hoijtink type in brackets, and orbital symmetry in parentheses within the brackets. [b] Calculated transition energy minus observed ($cm^{-1}$). [c] Experimental spectrum determined in this work. [d] Experimental spectrum from ref 15. [e] Experimental spectrum from ref 16. [f] Experimental spectrum from ref 17. [g] Experimental spectrum from ref 18. [h] Experimental spectrum from ref 21.

A and type B components.[22] The type A, type B band separation is calculated to be smallest for *p*-dicyanobenzene radical anion (**6**•−), and because both have $b_{2g}$ symmetry, there will obviously be significant configuration interaction, which is evident in the $\Delta E$ values shown in Table 2. The predicted energy of the low-energy band is one of the three most strongly overestimated, and the predicted high-energy band is the only one in this series that is underestimated. Apparently the CI effect is so large here that it overcomes the usual tendency to overestimate the higher band energies. Both dimethyl terephthalate (**7**•−) and terephthalaldehyde (**8**•−) are correctly predicted to be mixtures of s-cis and s-trans rotamers (the calculated cis, trans energy differences are 0.01 and 0.21 kcal/mol, respectively), as was shown earlier by ESR spectroscopy for the latter.[23] The isomers of **7**•− are predicted to have not only vanishingly small energy differences but also nearly identical optical spectra for its two isomers, and the experimental spectrum of **7**•− shows the largest first vibrational component and a vibrational structure in both bands that is consistent with essentially overlapping spectra. **8**•−, on the other hand, is predicted to have significantly different lowest transition energies for its rotamers, and the s-cis form is predicted to have detectable intensity at higher energy. The observed band shape is significantly different than for **7**•−, and is qualitatively consistent with this increase in spectral complexity. Fine structure has also been lost in the second band, for which the transition energies are calculated to differ by only 220 $cm^{-1}$; they presumably actually differ by more. The high-energy bands for **9**•− and **10**•− are predicted at considerably higher energy than those observed, which we note is also true for the compounds at the other extreme of the $B_i - A_i$ range (Table 1). It may well be that the actual transitions are significantly more complex than the simple predictions available using the Koopmans-based method. Nevertheless, we find the qualitative agreement of the spectra with this simple model quite striking.

## Conclusion

Despite its simplicity, the Koopmans-based model is useful for understanding the optical spectra of delocalized intervalence radical ions. Configuration interaction causes substantial shifts of the bands to lower energy. However, assignments can be made without considering configuration interaction, and the shifts observed can be considered as measures of the importance of configuration interaction in determining transition energies.

(21) Nelsen, S. F.; Konradsson, A. E.; Weaver, M. N.; Telo, J. P. *J. Am. Chem. Soc.* **2003**, *125*, 12493−12501.
(22) This point will be presented in full in a future paper on quinone radical anions.
(23) Maki, A. H. *J. Chem. Phys.* **1961**, *35*, 761.

**Acknowledgment.** We thank the National Science Foundation for partial financial support of this work under CHE-0240197 (S.F.N.), and Fundação Para a Ciência e Tecnologia for support through its Centro de Química Estrutural (J.P.T.). We thank Frank Weinhold (University of Wisconsin) for showing us how to obtain the band intensities for Koopmans-based transitions using his NBO program.

**Supporting Information Available:** Tables comparing Koopmans-based calculations with TD-DFT calculations that include the forbidden as well as the allowed transitions for compounds **1**−**10**, and orbital drawings for the orbitals involved in the more-intense transitions. This material is available free of charge via the Internet at http://pubs.acs.org.

JO0514218